Available online at www.sciencedirect.com
SCIENCE DIRECT®
Journal of Nuclear Materials 347 (2005) 151–160
journal of nuclear materials
www.elsevier.com/locate/jnucmat

Nickel boride (NiB) as an inhibitor for an IGSCC of Alloy 600 and its applicability

Yongsun Yi *, Seolhwan Eom, Hongpyo Kim, Joungsoo Kim

Korea Atomic Energy Research Institute, 150 Deokjin-dong, Yuseoung-gu, Daejeon 305-353, South Korea

Received 17 March 2005; accepted 23 August 2005

Abstract

Using an Alloy 600 tubing, slow strain rate tensile tests and polarization measurements have been performed in deaerated 40% sodium hydroxide and in aerated ammonia solutions (pH = ~ 9.5) at 315 °C. Tensile samples strained at an open circuit potential showed a severe intergranular stress corrosion cracking in the NaOH solution and small intergranular cracks were observed on the gage section of the samples tested in the ammonia solution. When added to both the solutions, borides were found to suppress the IGSCC. From the polarization curves in the NaOH solution with and without the additives, the corrosion current densities were estimated. The corrosion current density of the alloy in the 40% NaOH solution was significantly decreased by the addition of CeB_6 and NiB to the solution, which was judged to be attributed to the reduced corrosion current density. In the experiments, NiB showed a greater effectiveness for a corrosion and SCC inhibition than CeB_6.

PACS: 62.20.Mk

1. Introduction

Steam generator tubes in pressurized water reactors (PWRs) form a pressure boundary between the primary and secondary sides. Austenitic stainless steel was used initially for the tubing, but it was changed to Alloy 600 as the results of corrosion problems. Experiences with Alloy 600 in the late 1960s and early 1970s, in the early high temperature large PWRs, identified numerous corrosion problems. Efforts for the development of a new alloy were made and the result was Alloy 690. Since the mid-1980s new and replacement steam generators have used Alloy 690. However, PWRs with Alloy 600 steam generators are still being operated.

A lot of problems related to corrosion have been reported in Alloy 600 steam generator tubes of operating nuclear power plants (NPP), and the outer-diameter stress corrosion cracking (ODSCC) and intergranular attack (IGA) which have been occurring in Alloy 600 tubes are known to be the leading causes of PWR steam generator tube plugging in the USA and worldwide [1]. As reported by Diercks

* Corresponding author. Tel.: +82 42 868 8670; fax: +82 42 868 8549.
E-mail address: yongsunyi@kaeri.re.kr (Y. Yi).

0022-3115/$ - see front matter © 2005 Elsevier B.V. All rights reserved.
doi:10.1016/j.jnucmat.2005.08.011

et al. [1], the causes for a steam generator tube plugging have evolved with time and in recent years, ODSCC/IGA have become the predominant identifiable causes that lead to a plugging of steam generator tubes. It is known that the ODSCC mostly occurs in flow-restricted areas at the top of tube sheet or between the tubes and support plates (TSPs) [2]. Since the tube support plate crevice and sludge/tube crevice where the SCC occurs are mainly inaccessible, it is not easy to identify the exact chemistry causing the degradation. By using indirect methods such as a hideout return analysis, laboratory heated crevice testing, etc. many research programs for identifying the specific chemistries have been carried out [3,4]. Through the programs several possible causes have been suggested [5], but they are still debatable.

On the other hand, numerous studies for mitigating or avoiding the corrosion related problems in the steam generators have been carried out. It is clear that a tight adherence to the water chemistry guidelines is essential to keep IGA/SCC to a minimum but that as yet there are no reliable means to prevent a continued occurrence of IGA/SCC at affected plants [5]. One approach that has shown significant promise in laboratory tests is the use of chemical inhibitors [6]. Adding chemical inhibitors to the secondary side of the steam generators as a method that can be applied to currently operating plants has been extensively studied [7–10]. Recently, Hur et al. evaluated the effectiveness of inhibitors in terms of the crack depth on C-rings anodically polarized to 150 mV vs. the open circuit potential (OCP). They compared the effectiveness of TiO_2, TiB_2, and CeB_6 in the same condition and proposed cerium boride (CeB_6) as one of the most effective inhibitors [11]. This study was originally to verify the inhibition mechanism of boride. However, the exact inhibition mechanism is still questionable.

This paper focuses on the role of borides for an IGSCC inhibition for Alloy 600 in caustic solutions. To evaluate the effect of the borides on the SCC susceptibility of Alloy 600 in caustic solutions, SSRT tests were performed with Alloy 600 samples at the OCP in 40% NaOH and NH_3 solutions with and without borides. Also, in the same solutions, polarization curves were measured and the corrosion current densities were estimated using polarization curves. From the standpoint of the effectiveness of the inhibitor the experimental test results are discussed.

2. Experiment

2.1. Materials

Archived YGN 3&4 steam generator tubing with an outer diameter of 19.05 mm and a thickness of 1.07 mm was used. Chemical compositions of the Alloy 600 tubing used are given in Table 1. The Alloy 600 used in this study was high temperature mill-annealed (HTMA) at 1025 °C for 3 min.

2.2. SCC tests

To investigate the effect of chemical additives to the secondary side environment on the SCC behavior of Alloy 600 MA, SSRT (slow strain rate tensile) tests with tensile samples were performed. Tensile samples with a gage length of 25.4 mm, a gage width of 4 mm, and a thickness of 1.07 mm were machined from the archived YGN 3&4 steam generator tubing. The shape of the tensile test sample is shown in Fig. 1. SSRT tests were conducted in a static autoclave made of Alloy 625. For the SCC tests two reference solutions were chosen, (A) 40% NaOH and (B) ammonia (NH_3, $pH_{RT} = 9.5$–9.7) solutions. For a comparison, samples were tested in air. All the conditions for the SSRT tests are summarized in Table 2.

In the first group (Group A) the reference solution was a 315 °C 40% NaOH aqueous solution. The additives in this group were selected to isolate the effects of specific elements and were divided into three Subgroups; (A-1) cerium, (A-2) boron, and (A-3) boride. In Subgroup A-1, to exclude the effect of boron, two chemicals, CeO_2 and $(CH_3COO)_3Ce$, including cerium (III) and (IV) cations, respectively, were added to the reference solution. In the solutions containing H_3BO_3 and $Na_2B_4O_7$, it is expected that the effect of Ce on the SCC would be excluded (Subgroup A-2). In Subgroup A-3, two other borides, nickel and iron borides, were also selected and added to the reference solution. The concentration of H_3BO_3 in the solution was 20 g/l and that of the others was 2 g/l. Before straining the samples, the solution was continuously purged with pure nitrogen gas for 24 h. The tests in the aqueous solutions were performed at the strain rate of $1 \times 10^{-6}\ s^{-1}$. Surface appearance in the gage section and that of the fracture surfaces after the SSRT tests was examined with SEM.

In the second group (Group B), a 315 °C ammonia (NH_3) solution was the reference solution and

Table 1
Chemical compositions of Alloy 600 (wt%)

C	Ni	Cr	Fe	Ti	Al	Mn	Si	Co	Cu	N	B	P	S
0.026	72.4	16.81	9.01	0.36	0.16	0.83	0.33	0.01	0.01	0.018	0.001	0.007	0.001

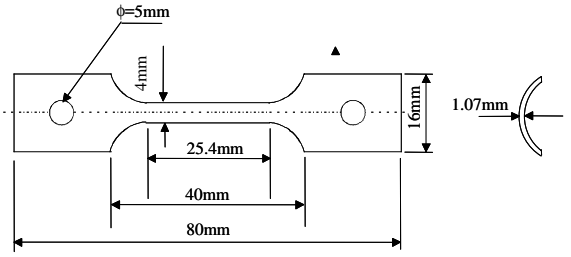

Fig. 1. Shape and dimensions of the test sample employed.

the pH of the solutions in this group was adjusted to between 9.5 and 9.7 by the addition of ammonia. Compared with the NaOH solution, the ammonia solution is much less aggressive. Therefore, the tests were performed in an aerated condition and the strain rate of the tests was $3 \times 10^{-7}\,s^{-1}$ to give the samples enough exposure time to crack. On the samples tested in the ammonia solutions, besides a SEM examination, AES depth profiles of the surface oxide composition were also measured with a PHI 680 Auger nano-probe operated at a primary beam energy of 5 kV and an electron current of 15–20 nA. Depth profiling of the surface oxide was performed using 1–4 keV argon ions.

In air, a faster strain rate of $1 \times 10^{-5}\,s^{-1}$ was selected since the strain rate in air has no influence on the mechanical properties over the range of interest. Tests in air were performed at room temperature and at 315 °C.

2.3. Polarization measurements

For the measurement of the polarization curves, coupons of 5 mm × 10 mm × 1 mm were machined from the above S/G tubes. The coupon surface was polished up to 0.1 μm using alumina paste and it was then spot-welded to an Alloy 600 wire. The polarization curves were potentio-dynamically measured in a 1 l volume static autoclave made of Ni using the Model 273 Potentiostat/Galvanostat (EG&G PAR). An external Ag/AgCl and the autoclave itself were used as the reference and counter electrodes, respectively. First, at −1.5 V vs. the open circuit potential (OCP), the samples were cathodically treated for 30 min to remove the oxides on the surface and then polarized from −1.5 to 1.5 V vs. OCP at a scan rate of 1 mV/s. In the SSRT tests and the polarization measurements, all the solutions were deaerated by a bubbling with pure nitrogen gas for 24 h.

3. Results and discussion

3.1. SSRT tests

3.1.1. NaOH solutions

Numerous studies have been performed to understand better the environment in the crevice where the ODSCC mainly occurs. Early studies that were

Table 2
SSRT test conditions

Reference solutions	Additives			Temperature (°C)	Strain rate (s^{-1})
(A) 40% NaOH	(A-1) Cerium CeO_2 $[Ce^{4+}]$	(A-2) Boron H_3BO_3 $[B(OH)_4^-]$	(A-3) Boride CeB_6	315	1×10^{-6}
	$(CH_3COO)_3Ce$ $[Ce^{3+}]$	$Na_2B_4O_7$ $[(B_4)O_7^{2-}]$	NiB FeB		
(B) NH_3 (pH = 9.5–9.7)			(B-1) Boride CeB_6 NiB	315	3×10^{-7}
(C) Air				20 315	1×10^{-5}

performed to evaluate the environment using hide-out return data and a computer code (such as MULTEQ) pointed out that a highly alkaline environment with a pH above 10 could cause the degradation. Recent studies have suggested that the degradation may occur in an environment nearly neutral or moderately alkaline [12]. Aqueous solutions with a pH higher than 10 have been frequently used in experiments related to the phenomenon. In this study, 40% NaOH solution, as a most severe condition, was used as the reference solution in the first group. It has also been known that the SCC susceptibility of Alloy 600 depends on the applied potential. Lumsden reported that in the pH 8 alumino-silicate solutions, SCC occurred at the potentials of 50 and 100 mV vs. OCP but that no cracking was found at the OCP and 150 mV vs. OCP [13]. It was found that, in the potential range between 150 and 200 mV above the OCP, Alloy 600 in a NaOH solution showed the highest SCC susceptibility [14,15]. Many experiments for evaluating the SCC susceptibility of Alloy 600 in caustic solutions have been performed at an applied potential between 150 and 200 mV above the open circuit potential (OCP) [9,11]. However, in the field the SCC phenomenon occurs at the open circuit potential of the alloy, so the effectiveness of an inhibitor should be evaluated for samples exposed to a caustic solution at the OCP as well as at a certain anodic potential. One disadvantage of the tests at OCP is that these usually take a long time since the crack initiation and propagation occur very slowly. In this study, to have IG cracks accelerated mechanically SSRT tests have been carried out using tensile samples without applying any potential to the samples.

Fig. 2(a) shows the stress–strain curves of Alloy 600 in a 40% NaOH solution at 315 °C along with a curve determined in air as a reference. In air, the ultimate tensile strength (UTS) of the alloy decreased at a higher test temperature but no apparent decrease in the elongation to a failure was observed between room temperature and 315 °C. The sample in a 40% NaOH solution failed at a shorter elongation than that in air. Fig. 2(b) shows the stress–strain curves of the alloy in 40% NaOH solutions containing various additives at 315 °C. It was shown in the figure that the curves of the alloy obtained in the solutions containing the additives were scattered around the curve measured in air. Fig. 3 is an SEM micrograph of the fracture surface of the sample tested in the reference solution (40% NaOH) showing an intergranular crack. IG cracks with a maximum depth of about 100 μm were observed along the sample's edge. From this observation the decrease in the elongation of the sample in the

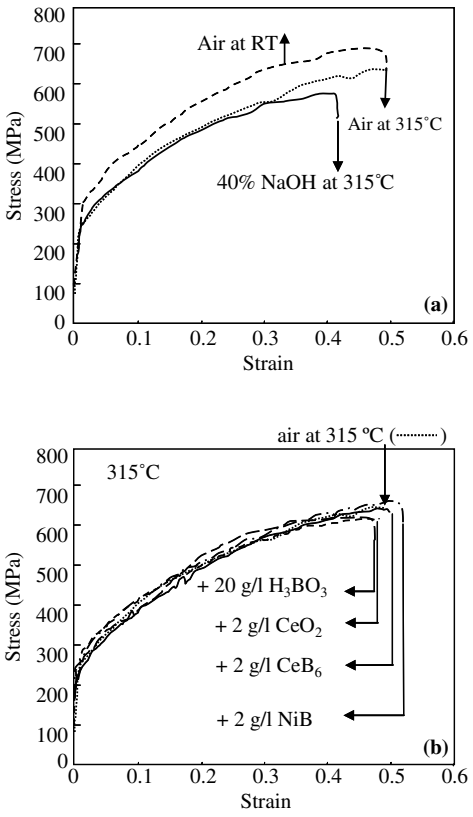

Fig. 2. The stress–strain curves obtained from the SSRT tests in (a) air and 40% NaOH solution and (b) the solutions containing additives.

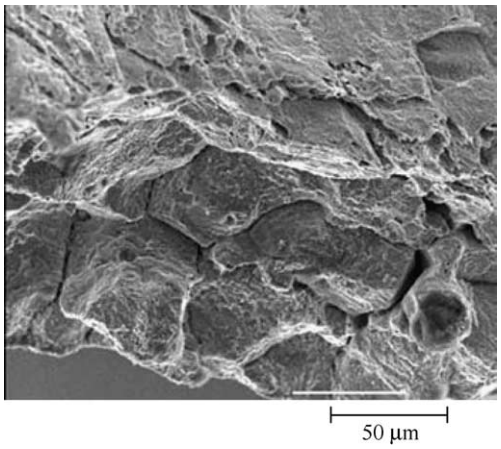

Fig. 3. SEM micrograph of the fracture surface of a sample strained in a 40% NaOH solution at 315 °C. On the sample IG cracks were observed along the edge.

reference solution is attributed to the IG cracking on the fracture surface. Based on this observation in Fig. 3 the SCC susceptibility of a sample could be quantitatively evaluated in terms of the elongation to failure from the SSRT tests [16]. However, except for the sample tested in the reference solution, the others did show only shallow IG cracks or no cracks on the fracture surface, resulting in no discernable difference in the elongation to a failure.

Fig. 4 shows the gage sections of the samples tested in all the solutions. First, widely opened IG cracks were observed on the gage sections of the sample tested in the reference solution (Fig. 4(a)). From this SEM micrograph and Fig. 4, it can be presumed that, in spite of the relatively fast strain rate, the caustic solution was enough to cause an IGSCC on Alloy 600. The gage sections of the samples tested in Subgroups A-2 and A-3 are shown in Fig. 4(a) and (c). In these SEM micrographs, a lot of

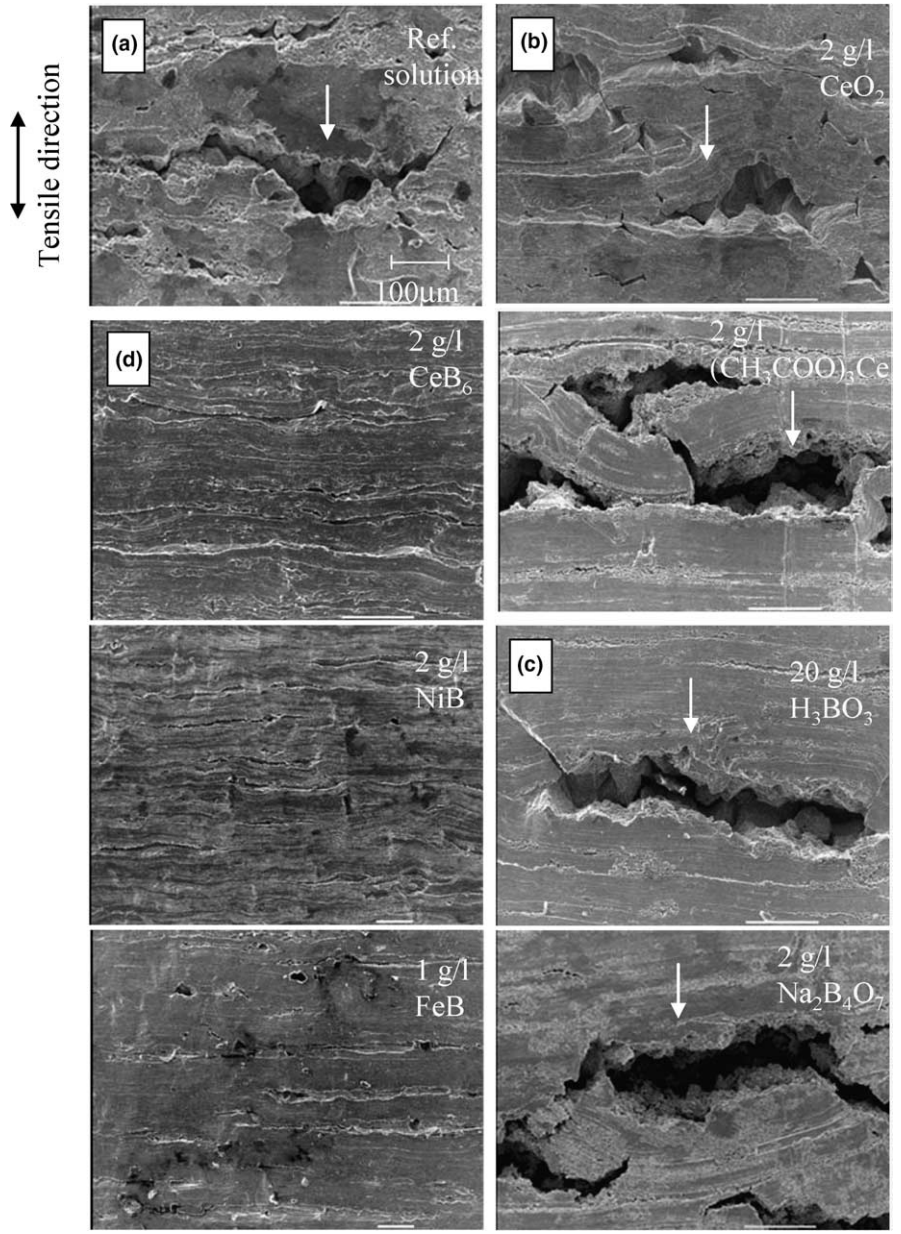

Fig. 4. SEM micrographs of the gage surface of samples strained in (a) a 40% NaOH solution (reference solution), (b) Subgroup A-1 (Ce), (c) Subgroup A-2 (B), and (d) Subgroup A-3 (boride) at 315 °C. White arrows indicate IG cracks.

IG cracks are observed, which suggests that cerium ions (Ce^{4+} or Ce^{3+}) and boron containing ions have little effect on the inhibition of an IGSCC in this caustic environment. Finally, in Fig. 4(d) except for very small cracks on the sample in FeB, no IG cracks were found on the samples tested in the boride containing solutions. This is very consistent with the results by Hur et al. [11] who reported that the borides (TiB_2 and CeB_6) enhanced the SCC resistance of Alloy 600 in a 10% NaOH solution. The inhibition effectiveness of the borides here could not be quantitatively compared since all the samples failed mechanically before the IG cracks grew sufficiently enough. However, the observation that the alloy did not crack in the boride containing solutions suggests that boride itself may play a role in the inhibition of an IGSCC of the alloy in the caustic solution.

3.1.2. Ammonia solution

Most PWRs used a coordinated phosphate treatment up to the early 1970s. However, as a result of the SCC and IGC sustained with a phosphate water treatment, the use of an AVT water treatment was initiated at most PWRs with recirculating steam generators (RSGs) and Alloy 600 MA tubing was used around about 1974 [17]. Ammonia is the pH reagent that was used mainly for the plants constructed up to the mid-1980s [18]. Since the mid-1980s morpholine or amines have been used in secondary water additives, but some nuclear power plants are still using ammonia.

The SSRT tests were performed in an ammonia solution to confirm the applicability of the borides to nuclear power plants that were found to suppress the IGSCC of Alloy 600 in the strong caustic (NaOH) solution. In order to verify the applicability of an inhibitor to the operating plants, tests should be performed in a simulated water chemistry condition of operating plants including the amount of dissolved oxygen. However, since the simulated water chemistry condition of operating plants is much less aggressive than the caustic solution discussed in the previous section, the SCC would not occur easily in the condition. Therefore, tests in this study have been performed in aerated solutions to accelerate the SCC. Although the results may not be able to provide proper information by which the applicability of inhibitors can be evaluated, they are expected to help us determine whether or not the borides are soluble in such a mild solution. It was judged that the borides were soluble in NaOH solutions since the alloy showed different corrosion and SCC behaviors in the boride containing solutions. To determine the solubility of the borides to NPPs, SSRTs have been performed in an ammonia solution as the reference solution (Group B). Any changes in the corrosion or IGSCC behavior of the alloy by the addition of the borides would be an indication about whether or not the borides could be dissolved in the ammonia solutions.

Fig. 5 shows the stress–strain curves of the alloy determined in the ammonia solution with and without the borides. Owing to an error of the data acquisition system the recording for the sample in the NiB containing solution was interrupted in the middle of the test. Post-measurement of the sample length showed that the elongation to a failure of the sample was comparable to the others. No remarkable differences in the UTS and the elongation to a failure among the curves were observed. Fig. 6 shows SEM micrographs of the gage sections of the samples tested in the ammonia solution and the ammonia solutions containing CeB_6 and NiB. Only the sample tested in the ammonia solution without any additives showed small IG cracks and no IGSCC occurred on the other samples tested in the solution containing CeB_6 and NiB. The surface oxides were analyzed by an AES. In the compositions of the oxides no differences that deserve attention were found among the three samples (Fig. 7). Using the AES analysis results, the thickness of the surface oxides was estimated and it is summarized in Fig. 8. By the addition of the borides the thickness of the surface oxide was decreased and the addition of NiB resulted in the thinnest oxide. The SEM micrographs (Fig. 6) and the estimated oxide thickness of the samples (Fig. 8) imply that

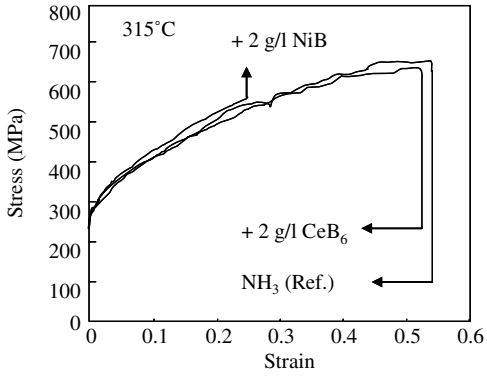

Fig. 5. Stress–strain curves obtained from the SSRT tests in ammonia solutions.

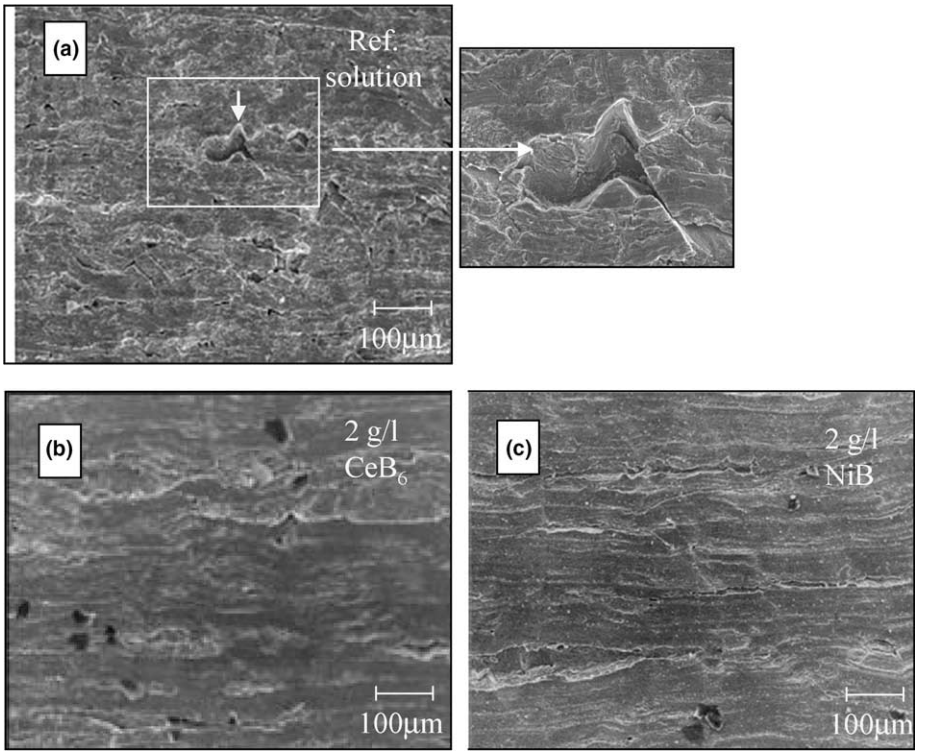

Fig. 6. SEM micrographs of the gage lengths of the samples tested in (a) the reference solution (NH_3, pH = 9.5) (b) Ref. + 2 g/l CeB_6 (pH = 9.7), and (c) Ref. + 2 g/l NiB (pH = 9.7).

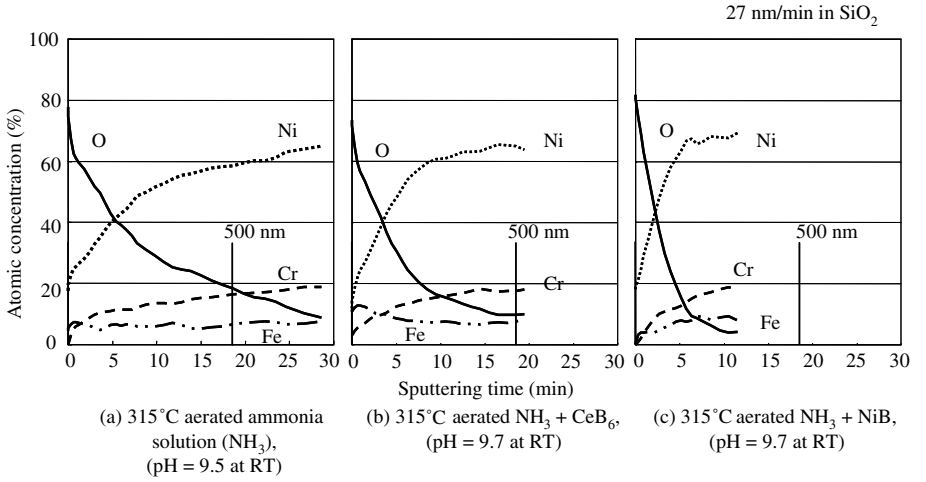

Fig. 7. AES depth profile of the surface oxides for the samples tested in the 315 °C ammonia solutions.

the boride can be applied to nuclear power plants. Also, the comparison of the oxide thickness suggests that NiB may be able to inhibit the corrosion of the alloy in an ammonia solution more effectively than CeB_6.

3.2. Polarization measurements

To identify the reproducibility of the polarization curves, the measurements were performed for two or more samples in one solution condition. The

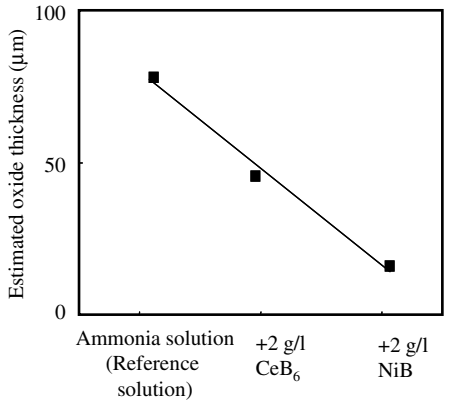

Fig. 8. Estimated surface oxide thickness of the samples tested in (a) the reference solution (NH_3, pH = 9.5) (b) Ref. + 2 g/l CeB_6 (pH = 9.7), and (c) Ref. + 2 g/l NiB (pH = 9.7).

potentio-dynamic polarization curves of Alloy 600 obtained in the reference solution and the 40% NaOH solutions containing CeB_6, NiB, and CeO_2, respectively, in Fig. 9. Some scatter in the OCPs and the active–passive transition potentials were found in the polarization curves determined in each test condition. The scatter in the potentials is thought to be due to the instability of the reference electrode and the high temperature condition. It was shown that plotted against the OCP and compared with each other, the curves obtained in each solution showed the same active–passive behaviors with no big difference in the peak and passive current densities. Based on this, the current densities in the curves were judged to be valid. However, the effect of the additive on the values of the OCP and the transition potential cannot be discussed due to the original scatter. The addition of CeB_6, NiB, and CeO_2, was found to reduce the active potential range. In the solutions containing the two kinds of boride the active peak current densities decreased while CeO_2 did show no effect on the peak current density. The significant decreases in the active potential range and the peak current density imply that, in the solution containing the two kinds of boride, surface passive film on the alloy could be formed more easily than in the reference solution.

In this study, the corrosion resistance of the alloy in each solution was evaluated in terms of the corrosion current density at the OCP. The corrosion current densities were estimated using 'the four point method' proposed by Jankowski and Juchniewicz [19]. In this method, four current density values (see Fig. 10) at four applied potentials, $E = \Delta E$, $-\Delta E$, $2\Delta E$, and $-2\Delta E$ on a polarization curve are used to determine the corrosion current density (I_{corr}), the harmonic mean of the Tafel constants (B), and of that each Tafel constant (b_a and b_c). The corrosion current density, I, is determined from the following equation:

$$I = \frac{I_1 I_{-1}}{\sqrt{I_2 I_{-2} - 4 I_1 I_{-1}}}, \tag{1}$$

where I_1, I_{-1}, I_2, and I_{-2} are the current densities at the four overpotentials, ΔE, $-\Delta E$, $2\Delta E$, and $-2\Delta E$ (see Fig. 10). The results obtained for the estimation of the corrosion current density are summarized in Table 3 and graphically in Fig. 11 along with the SEM micrographs of the gage length surface after

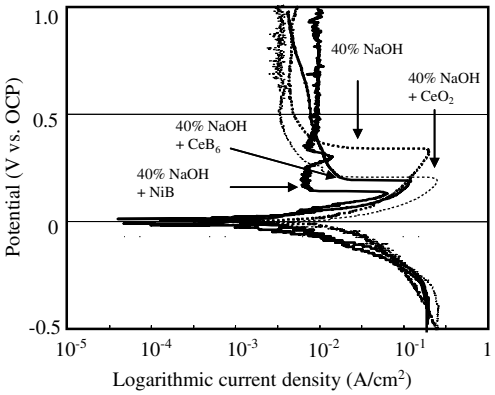

Fig. 9. Polarization curves of Alloy 600 in 40% NaOH solution with and without additives at 315 °C. The sweep rate was 1 mV/s.

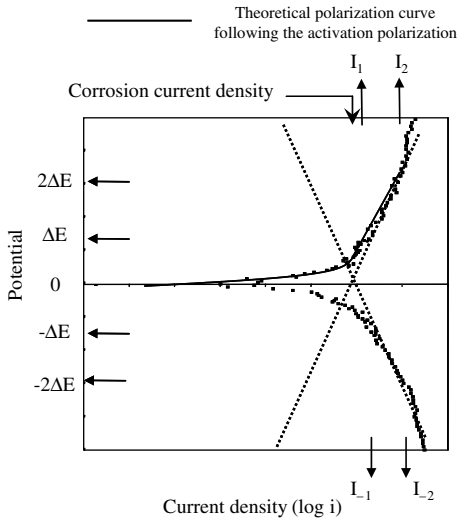

Fig. 10. Current densities used to determine the corrosion current density in the four point method.

Table 3
Corrosion current densities estimated using the four point method

Solution	Reference solutions	CeO_2	CeB_6	NiB
Current density (mA/cm^2)	21.3 ± 2.7	33.1 ± 14.8	2.5 ± 0.2	1.7 ± 0.3

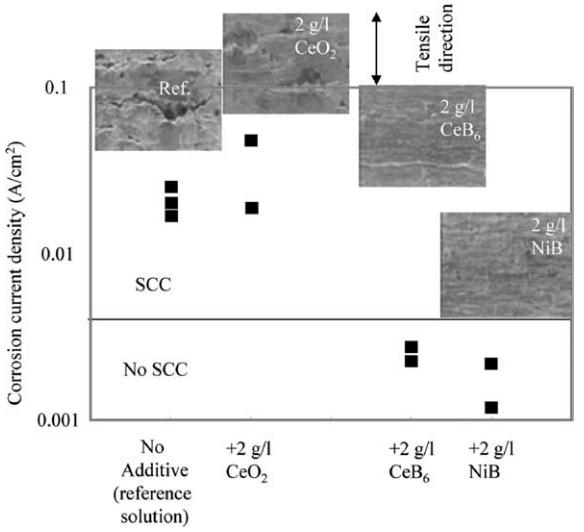

Fig. 11. The values of the corrosion current density in the various solutions along with the SEM micrographs of the gage surfaces in the same solutions showing the presence or absence of IG cracks.

the SSRT tests in the A group solutions. The corrosion current density of the alloy in the 40% NaOH solution was decreased by almost one order of the magnitude by the addition of the borides. The cerium oxide that had no effect on the SCC susceptibility showed comparable corrosion current densities to that of the reference solution. From this figure, it can be concluded that borides could enhance significantly the corrosion resistance of the alloy in a caustic solution.

3.3. SCC inhibition

The slip dissolution mechanism [20] is known to be the most feasible mechanism for the ODSCC of Alloy 600 tubing, in which the repassivation kinetics of the surface oxide governs the crack growth behavior. In this study, the repassivation behavior of the oxide in the solutions was not measured. However, Fig. 9 could give circumferential information about the repassivation behavior of the alloy in the solutions. The addition of the borides decreased the active potential range and the peak current density, implying that surface oxide on the alloy could be formed more easily. In the slip dissolution mechanism, the crack growth rate depends on the amount of the electric charge by mainly metallic dissolution during the repassivation. Based on this, it can be concluded that the IGSCC of the alloy was suppressed since the alloy could be passivated more easily by the addition of the borides. Among the borides used in this study NiB showed superior effectiveness of the corrosion inhibition as shown in Figs. 8 and 11.

With the efforts to develop proper corrosion inhibitors, their inhibition mechanisms have been investigated on this topic. Boric acid is known to be able to neutralize alkaline chemistry [18]. Kim et al. have shown that when TiO_2 is in a caustic solution, Ti ions are incorporated into the surface oxide, resulting in the enhancement of the repassivation of Alloy 600 [8]. The borides used in this study do not seem to play a role in a form of metallic ions or boron ions. This study showed that the borides themselves rather than ions might have inhibited the corrosion and SCC of the alloy. How the borides could make the surface oxide formation easier is unknown, which should be addressed in the further study. Also, the inhibition effectiveness of NiB should be evaluated in other solutions containing lead or reduced sulfur species since they are known to be deleterious in the secondary side condition [21–23].

4. Conclusions

(1) In the SSRT tests in 40% NaOH and ammonia (pH = 9.5–9.7) solutions at 315 °C, IGSCC occurred in Alloy 600 but when NiB or CeB_6 was added to the solution, the samples failed in a completely ductile manner, which leads to a conclusion that borides can suppress the IGSCC of Alloy 600 in strong caustic solutions.
(2) The corrosion current density of Alloy 600 was significantly decreased by the addition of the borides to the 40% NaOH solution and the addition of NiB had the maximum inhibition effect among borides used in this study.
(3) The absence of SCC on the fracture surface of the alloy tested in the solution containing borides is attributed to the reduced corrosion rate. A comparison between SCC behavior and the

measured corrosion current densities suggests that the SCC susceptibility can be evaluated in terms of the anodic corrosion current density.

(4) This study showed a possibility that NiB may be applied to the nuclear power plants.

Acknowledgment

This work was carried out as a part of the Steam Generator Materials Project under the Nuclear R&D Program sponsored by MOST in Korea.

References

[1] D.R. Diercks, W.J. Shack, J. Muscara, Nucl. Eng. Des. 194 (1999) 19.
[2] F. Vaillant, A. Stutzman, in: Proceedings of the 10th International Conference on Environmental Degradation of Materials in Nuclear Power Systems – Water Reactors, 5–9 August 2001, Lake Tahoe, Nevada.
[3] J.P.N Paine, S.A. Hobart, S.G. Sawochka, in: Proceedings of the 5th International Conference on Environmental Degradation of Materials in Nuclear Power Systems – Water Reactors, 25–29 August 1991, Monterey, California, p. 739.
[4] R.F. Voelker, in: Proceedings of the 10th International Conference on Environmental Degradation of Materials in Nuclear Power Systems – Water Reactors, 5–9 August 2001, Lake Tahoe, Nevada.
[5] J.A. Gorman, J.E. Harris, R.W. Staehle, K. Fruzzetti, in: Proceedings of the 11th International Symposium on Environmental Degradation of Materials in Nuclear Power Systems – Water Reactors, 10–14 August 2003, Stevenson, Washington, p. 362.
[6] S.G. Sawochka, R. Pearson, D.C. Gehrke, M. Miller, Experience with inhibitor injection to combat IGSCC in PWR steam generators, EPRI ReportTR-105003, (1995).
[7] J. Daret, J.P.N. Paine, M.J. Partridge, in: Proceedings of the 7th International Symposium on Environmental Degradation of Materials in Nuclear Power Systems – Water Reactors, 6–10 August 1995, Breckenridge, Colorado, p. 177.
[8] U.C. Kim, K.M. Kim, J.S. Kang, E.H. Lee, H.P. Kim, J. Nucl. Mater. 302 (2002) 104.
[9] H. Kawamura, H. Hirano, M. Koike, M. Suda, Corrosion 58 (2002) 941.
[10] M.J. Partridge, W.S. Zemitis, J.A. Gorman, Correlation of Secondary-Side IGA/SCC Degradation of Recirculating Steam Generator Tubing with the On-Line Addition of Boric Acid, EPRI Report TR-101010s (1992).
[11] D.H. Hur, J.S. Kim, J.S. Baek, J.G. Kim, Corrosion 58 (2002) 1031.
[12] A.M. Lancha, D. Gómez-Briceño, M. Garcia-Mazario, C. Maffiotte, in: Proceedings of the 8th International Symposium on Environmental Degradation of Materials in Nuclear Power Systems – Water Reactors, 10–14 August 1997, Amelia Island, Florida, p. 27.
[13] J. Lumsden, A. McIlree, in: Proceedings of the 11th International Symposium on Environmental Degradation of Materials in Nuclear Power Systems – Water Reactors, 10–14 August 2003, Stevenson, Washington, p. 458.
[14] B.P. Miglin, J.P. Paine, in: Proceedings of the 6th International Symposium on Environmental Degradation of Materials in Nuclear Power Systems – Water Reactors, 1–5 August 1993, San Diego, California, p. 303.
[15] J.B. Lumsden, J.P.N. Paine, in: Proceedings of the 7th International Symposium on Environmental Degradation of Materials in Nuclear Power Systems – Water Reactors, 7–10 August 1995, Breckenridge, Colorado, p. 317.
[16] M. Popovic, E. Romhanji, J. Mater. Process. Technol. 125–126 (2002) 275.
[17] R.W. Staehle, J.A. Gorman, in: Proceedings of the 10th International Conference on Environmental Degradation of Materials in Nuclear Power Systems – Water Reactors, 5–9 August 2001, Lake Tahoe, Nevada.
[18] F. Nordmann, J.-M. Fiquet, Nucl. Eng. Des. 160 (1996) 193.
[19] J. Jankowski, R. Juchniewicz, Corros. Sci. 20 (1980) 841.
[20] P.L. Andresen, F.P. Ford, Mater. Sci. Eng. 103 (1988) 167.
[21] O.de Bouvier, E-M. Pavageau, F. Vaillant, D. Vermeeren, in: Proceedings of the 11th International Symposium on Environmental Degradation of Materials in Nuclear Power Systems – Water Reactors, 10–14 August 2003, Stevenson, Washington, p. 467.
[22] D. Costa, H. Talah, P. Marcus, M. Ls Calvar, A. Gelpi, in: Proceedings of the 7th International Symposium on Environmental Degradation of Materials in Nuclear Power Systems – Water Reactors, 7–10 August 1995, Breckenridge, Colorado, p. 199.
[23] R.W. Staehle, in: Proceedings of the 11th International Symposium on Environmental Degradation of Materials in Nuclear Power Systems – Water Reactors, 10–14 August 2003, Stevenson, Washington, p. 381.